*Eur J Med Chem* (1992) 27, 825–833



# A study of the delivery-targeting concept applied to antineoplasic drugs active on human osteosarcoma. I. Synthesis and biological activity in nude mice carrying human osteosarcoma xenografts of gem-bisphosphonic methotrexate analogues

G Sturtz[1], G Appéré[1], K Breistol[2], O Fodstad[2], G Schwartsmann[3], HR Hendriks[3]

[1]*Laboratoire de Chimie Hétéro-Organique, Université de Bretagne Occidentale, 6, avenue Le Gorgeu, 29275 Brest Cedex, France;*
[2]*Department of Tumor Biology, The Norwegian Radium Hospital, Oslo, Norway;*
[3]*EORTC New Drug Development Office, Free University Hospital, Amsterdam, The Netherlands*

(Received 25 November 1991; accepted 24 June 1992)

**Summary** — With the aim of verifying the concept of osteotic vectorisation, synthesis of three methotrexate (MTX) gem-diphosphonic analogues (compounds **A**, **B** and **C**) was performed. These molecules were tested on BALB/c and NIH III mice previously grafted with subcutaneous implants of OHS, TTX p7 and/or TTX p11 human osteosarcoma cell lines. Antineoplasic activity of compound **B** and **C** (active compounds) was compared to the activity for MTX alone and to activity of compound **A** (inactive compound). Compounds **B** and **C** exhibited an increased antineoplasic activity compared to MTX alone and to compound **A**. At equimolar doses, compound **B** was found to be 5–6-fold more active than MTX given alone. We have discussed the concept of osteotic vectorisation of compound **B**, which could be regarded as a prodrug.

**gem-bisphosphonic synthesis / methotrexate / antineoplasic activity / osteosarcoma / delivering targeting concept**

## Introduction

Methotrexate (MTX) is a well-known antifolate agent (fig 1), which has shown significant antitumor activity in human bone sarcomas [1]. Single agent high-dose MTX can produce objective response rates in about 30–40% of patients with metastatic disease [2]. Therefore, this type of therapy has been widely used in experimental protocols of neoadjuvant therapy, followed by limb-sparing procedures [3]. The main dose-limiting toxicities of MTX are myelosuppression, mucositis and diarrhoea [4].

Bisphosphonates absorb to bone [5, 6] and are used clinically to treat hypercalcemia [7] and tumor-induced osteolysis [8]. Conjugates of cytostatic agents and bisphosphonates represent a new class of compounds in which the bisphosphonate moiety is used as a carrier to bone. Such conjugates maintain both osteotropic and cytotoxic properties [9]. Considering the potential of bisphosphonates to accumulate in bone matrix [6], and recent studies which have brought to light the important role played by the metabolic transformation of MTX into its polyglutamate derivative (MTX PGS) for the cytotoxic effect [11], we have synthetized three MTX analogues (compounds **A**, **B** and **C**) with the aim of increasing drug localization in osteoid-producing tumors. The antineoplasic activity of these compounds and of MTX alone was tested on the osteosarcoma cell lines OHS and TTX growing subcutaneously as xenografts in BALB/c and NIH III nude mice.

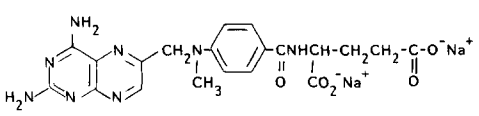

**Fig 1.** Methotrexate.

These MTX-analogues (compounds **A**, **B** and **C**) present a MTX-like part and gem-diphosphonate part. Compound **A** [10] (fig 2) could be considered as an ineffective drug since the MTX-like moiety is incomplete while compound **B** (fig 3) and **C** (fig 4), comprising a full MTX-like moiety, could be regarded as delivery-targeted prodrugs.

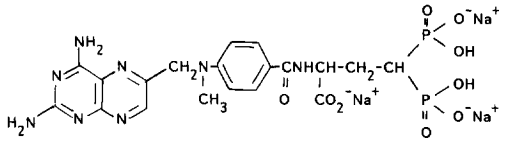

**Fig 2.** Compound **A**.

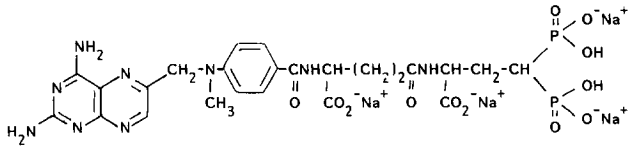

**Fig 3.** Compound **B**.

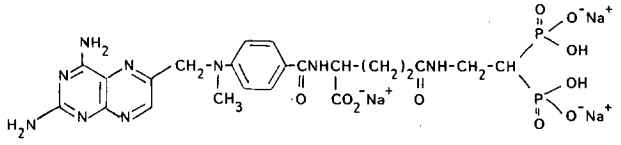

**Fig 4.** Compound **C**.

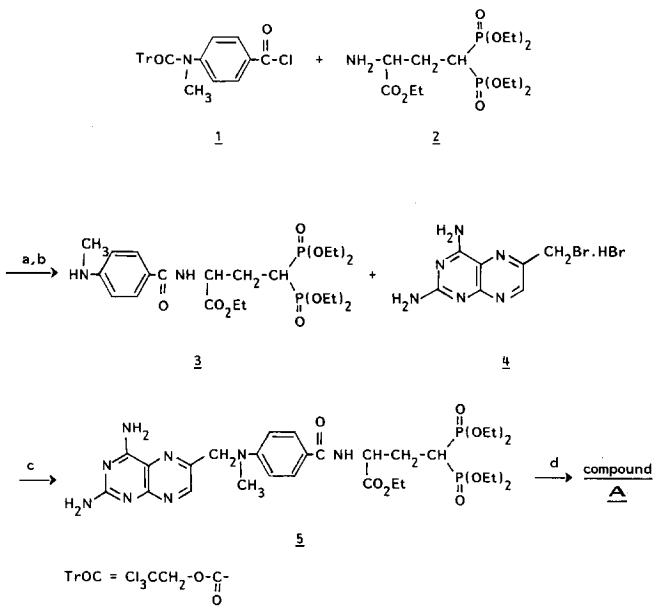

**Scheme 1.** Synthesis of compound **A**. Reaction conditions: (a) $Et_3N$/THF; (b) Zn/$KH_2PO_4$/pH 4–5; (c) DMA heating 50°C; (d) 1) $(CH_3)_3SiBr$; 2) $CH_3OH$; 3) NaOH.

## Chemistry

*Synthesis of compound A*

This compound has been previously described [10]. We propose here a new strategy based on the convergent synthesis principle, which allows the synthesis of new useful intermediates involved in the synthesis of compounds **B** and **C**. Using procedures reported by Piper and Montgomery [12] the following synthetic sequence was investigated (scheme 1).

The diphosphonate **3** was prepared by condensation of ethyl 2-amino 4,4-bis(diethylphosphono)butyrate **2** on the protected form of the *p-N*-methylamino benzoic acid chloride.

The protecting group was then removed at controlled pH using zinc powder as reagent. The nucleophilic substitution, involving the 6-bromomethyl 2,4-diaminopteridine derivative was directly performed at 50°C in dimethyl acetamide (DMA) as solvent without protection of the amine functions of the pteridin moiety [13] as there was no need for trapping bromhydric acid by an auxiliary base [12]. Hydrolysis of the phosphonic ester functions was carried out using trimethylsilyl bromide [14] as reagent, followed by methanolysis. After saponification, isolation of the final compound **A** was possible.

*Synthesis of the prodrug B*

The most satisfactory synthesis was the following (scheme 2): glutamic acid benzyl ester **6** (prepared according to the procedure reported in [15]) was N-protected as the urethane intermediate **7** using diterbutyldicarbonate. The coupling step between **7** and 2-amino 4,4-bisdiethylphosphonobutyrate ethyl ester **2** was achieved using dicyclohexylcarbodiimide (DCC) leading to compound **8**, which upon treatment with trifluoroacetic acid gives the corresponding amino gem bisphosphonic ester **9**. Condensation of **9** with the protected *p-N*-methylaminobenzoic acid chloride, led after zinc provided amino-group deprotection, to the intermediate **10**. Compound **10** was then heated in DMA at 50°C with 6-bromomethyl 2,4-diaminopteridine **1**, giving the esterified form **11** of compound **B**. Final compound **B** was obtained by selective hydrolysis of the phosphonic ester functions using trimethylsilyl bromide followed by a subsequent methanolysis and saponification of carboxylic ester function.

*Synthesis of the prodrug C*

The following strategy, described in scheme 3, has been developed from glutamine **12**, whose amino group was initially protected as N-BOC using diterbutyl dicarbonate in dioxane, which was esterified by reacting ethyl iodide in DMF in the presence of diisopropyl ethylamine.

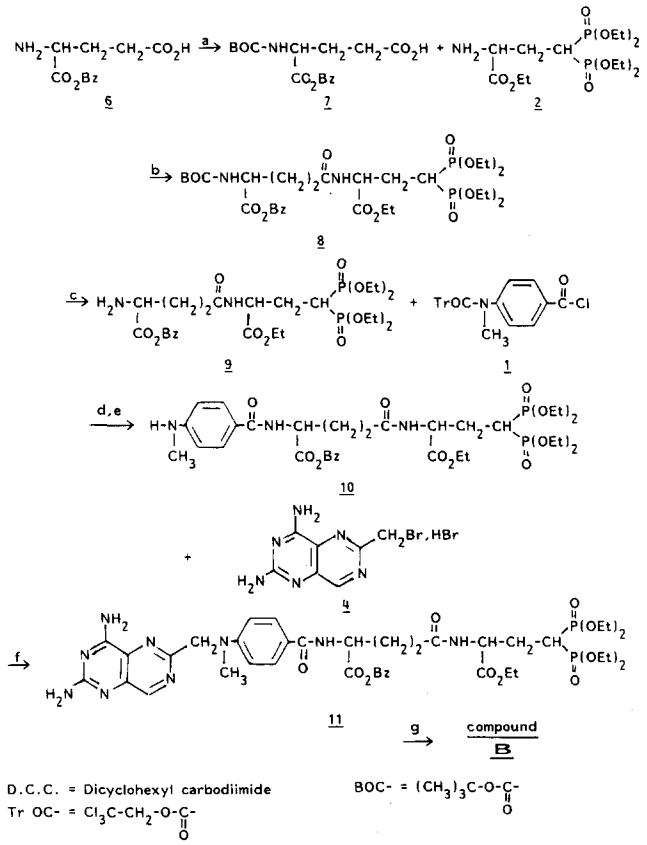


**Scheme 2.** Synthesis of compound **B**. Reaction conditions: (a) $(BOC)_2O$; (b) DCC; (c) TFA; (d) $Et_3N$/THF; (e) $Zn/KH_2PO_4$ pH 4–5; (f) DMA heating 50°C; (g) 1) $(CH_3)_3SiBr$; 2) $CH_3OH$; 3) NaOH.

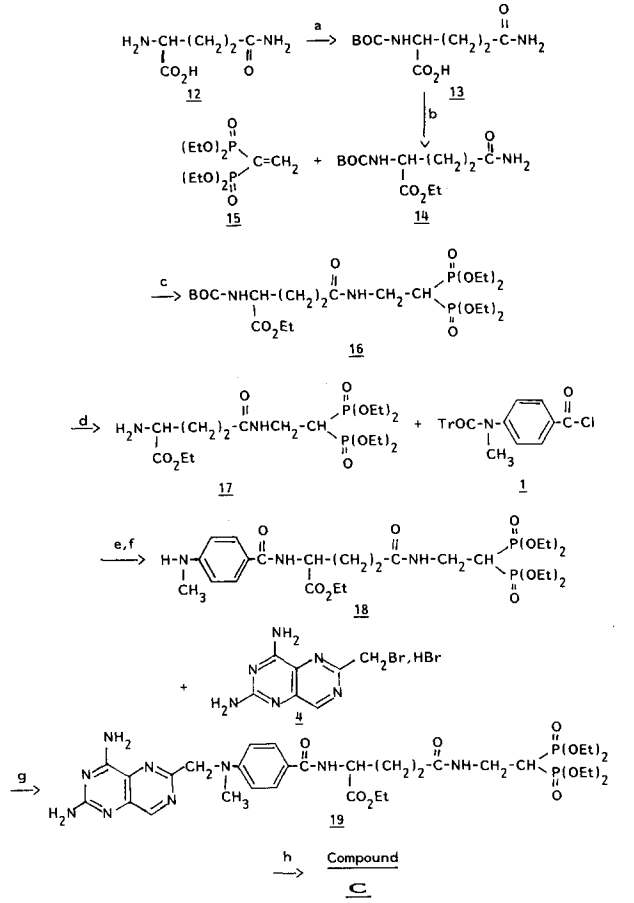


**Scheme 3.** Synthesis of compound **C**. Reaction conditions: (a) $(BOC)_2O$; (b) $C_2H_5I$-$(iPr)_2EtN$/DMF; (c) $tBuO^-K^+$/tBuOH; (d) $CF_3COOH$; (e) $Et_3N$/THF; (f) $Zn/KH_2PO_4$, pH 4–5; (g) DMA heating 50°C; (h) 1) $(CH_3)SiBr$, 2) $CH_3OH$, 3) NaOH.

As visualized by thin layer chromatography (TLC), the reaction rate at room temperature was very slow (4 days) to achieve the desired compound **14**. Through a Michael addition, using potassium terbutoxide in tertiobutanol, involving the diethyl vinylidene diphosphonate **15**, compound **16** was isolated. After treatment of **16** with trifluoro acetic acid in order to remove the N-BOC protecting group, the intermediate **17** was recovered. When **17** was condensed on the protected form **1** of *p-N*-methylaminobenzoic acid chloride, followed by zinc powder deprotection, the analogue **18** was isolated. Condensation of **18** at 50°C in DMA as solvent on the 6-bromomethyl 2,4-diaminopteridine substrate **4** led to compound **19**. Subsequent selective hydrolysis of the phosphonic ester functions using trimethylsilyl bromide followed by methanolysis and saponification of carboxylic ester function gave the final desired compound **C**.

## Pharmacology

Dose-finding studies were carried out in order to establish the MTD for compounds **A**, **B**, and **C**. The compounds were solubilized in Locke and injected iv into non-tumor-bearing nude mice (2–4 mice/dose level) days 0 and 7 at dose levels ranging from 50–200 mg/kg/injection. After dosing, body weight and toxic death were recorded. The median body weight from each group was determined daily.

The highest doses of the compounds caused rapid death of the mice, *viz ie* almost immediately after the first or second injection. Typically, mice receiving high doses developed a characteristic black colour on both the tail and the hind portion of the body. On the basis of numbers of toxic deaths and body weight loss in non-tumor-bearing nude mice, the following dose

was selected for use in therapy experiments in nude mice carrying xenografts: **A** and **B**, 100 mg/kg/injection, **C**, 75 mg/kg/injection.

The *in vivo* antitumor activity of the compounds was tested against human osteosarcomas, TTX and OHS, growing subcutaneously in the flanks of animals. Both lines showed a morphology closely similar to that seen in the patients of origin. The OHS xenografts regularly produce osteoid [21], whereas this is rarely seen in TTX tumors. During the therapy experiments both the dose and schedule had to be adjusted for compound **B**, because of large body weight loss and poor general conditions of the mice after the first drug injection.

The MTD for methotrexate was found to be 200 mg/kg when administered either by ip or iv routes. Since in most previous MTX experiments the ip route was used, this route was also chosen in the present study.

## Results and discussion

Two different numerical criteria were used for evaluation of antitumor effect, *viz* specific growth delay (SGD) and optimal growth inhibition (T/C %), and, in addition, tumor growth curves were constructed for visual assessment of activity (for details, see *Experimental protocols, Pharmacological evaluation*).

As can be seen in table I, compound **A** had virtually no effect in the three experiments performed. This finding was not surprising, since the conjugate contains an incomplete MTX moiety (fig 2). In contrast, compound **B** showed significant activity on tumor growth in all three experiments. Optimal tumor growth inhibition of OHS and TTX p7 was 21 and 15% respectively, with an SGD value (1–2) of 4.6 and 3.7. In comparison, free MTX (150 mg/kg) produced T/C values of 48 and 35% (SGD 1.0 and 1.2) in the same tumors. In both experiments, compound **C** was slightly less active than compound **B**. In the last experiment (TTX p11), compound **B** was given at two lower concentrations (40 mg/kg and 50 mg/kg), and the effects compared to that of MTX given at 200 mg/kg. In this case, MTX was slightly more effective than compound **B** for which indication of dose dependency was observed (table I).

The tumor volume growth curves for the TTX p7 experiments are shown in figure 5. Closely similar and moderate effects were seen for compound **C** and MTX, whereas coumpound **A** did not reduce the tumor growth rate. For the most active agent, compound **B**, the lowest tumor volumes were

**Table I.** Efficacy of compounds **A**, **B**, **C** (iv) as compared to MTX (ip) against human osteosarcoma xenografts implanted sc into nude mice.

| *Tumor type* | *Compound* | *Mouse strain* | *Dose (mg/kg)* | *Schedule* | *Number tumors* | *Max bw[a] loss (%)* | *Toxic death* | *Optimal T/C* % | *Day* | *SGD 1–2* | *1–4* | *Rating[c]* |
|---|---|---|---|---|---|---|---|---|---|---|---|---|
| OHS | **A** | BALB/c | 100 | d0,7 | 5 | 0 | 1/5 | 63 | 14 | 0.5 | 0.3 | – |
| | **B** | ♀♀ | 75/60 | d0,10 | 6 | 22.4 | 0/5 | 21 | 14 | 4.6 | 1.7 | +++ |
| | **C** | | 75 | d0,7 | 6 | 14.1 | 0/5 | 27 | 14 | 3.2 | 1.2 | ++ |
| | MTX | | 150 | d0,7 | 6 | 0 | 0/5 | 48 | 14 | 1 | 0.6 | (+) |
| TTX p7 | **A** | BALB/c | 100 | d0,7 | 8 | 0.4 | 2/7 | 81 | 27 | 0 | 0 | – |
| | **B** | ♂♂ | 100/75 | d0,10 | 11 | 2.4 | 0/7 | 15 | 17 | 3.7 | 2.4 | +++ |
| | **C** | | 75 | d0,7 | 12 | 4.1 | 0/8 | 32 | 20 | 1.8 | 1.1 | ++ |
| | MTX | | 150 | d0,7 | 12 | 1.7 | 0/8 | 35 | 17 | 1.2 | 1.1 | + |
| TTX p11 | **B**[b] | BALB/c | 40 | d0,7 | 13 | 0 | 0/7 | 64 | 3 | 1.0 | 0.2 | (+) |
| | **B**[b] | ♀♀ | 50 | d0,7 | 14 | 4.1 | 0/8 | 37 | 17 | 2.0 | 0.8 | ++ |
| | MTX | | 200 | d0,7 | 14 | 1.7 | 0/8 | 26 | 20 | 4.5 | 1 | ++ |

[a]Maximum body weight loss. [b]Compound in 0.9% NaCl. [c]Activity rating:

| | T/C% | | SGD |
|---|---|---|---|
| (+) | < 50% | or | > 1.0 |
| + | < 50% | and | > 1.0 |
| ++ | < 40% | and | > 1.5 |
| +++ | < 25% | and | > 2.0 |
| ++++ | < 10% | and | > 3.0 |

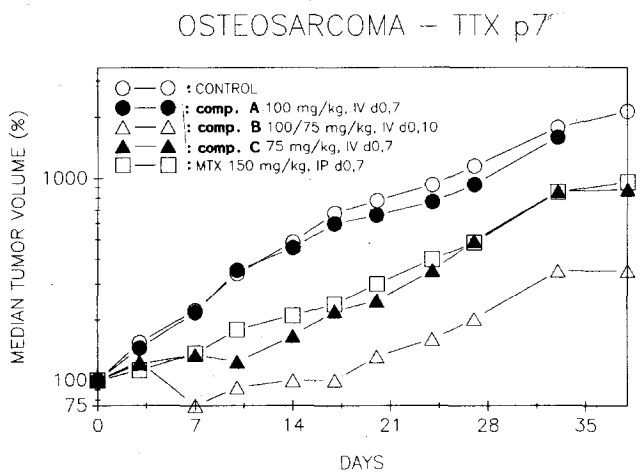


**Fig 5.** Tumor volume growth curves for the TTX p7 experiments.

measured on day 7, at which time the tumors were smaller than at the start of treatment. Although a moderate increase in tumor size was seen over the next 10 days, the tumors in this group of mice did not reach their original size until after about 18 days, after which time all the growth curves were parallel.

The degree of toxicity of the various agents on the hosts is indicated by the number of toxic deaths and by the maximum body weight loss (table I). Toxic deaths were seen in only three animals receiving compound **A**, which had no effect on tumor growth. In the OHS experiment, compounds **B** and **C** produced significant weight loss compared to MTX. In the two other experiments, however, no clear differences were seen.

The experience with compound **B** in tumor-bearing mice indicates that its MTD, given at a day 0 and 7 schedule, is about 50–75 mg/kg, compared to 200 mg/kg for MTX (not shown). The data do not permit a definite conclusion as to whether the activity of compound **B** is superior to that of MTX at equitoxic doses, but overall the results suggest that this is the case. Moreover, it is clear that on a molar basis 5–6-fold more MTX (MTD 200 mg = 0.41 mmol) was needed to obtain similar antitumor activity as that obtained with compound **B** (50–75 mg = 0.07 mmol).

The present results demonstrate that by conjugating MTX to bisphosphonate it is possible to obtain increased cyctotoxicity (compound **B**) against human osteosarcoma tumors *in vivo*. Interestingly, that this novel treatment modality was successful *in vivo* could not be predicted by *in vitro* tests, as antineoplastic activities of compound **B**, **C** and MTX alone were not significantly different in an *in vitro* test system (Braakhuis, unpublished data).

The 3 conjugates (**A**, **B**, **C**) which showed significant differences in activity, differ in their linkage between MTX and the other chemical moiety. In addition, compound **A** did not contain a complete MTX molecule. The observed difference in potency between **B** and **C** may possibly be explained in terms of different targeting capabilities. Moreover, the dissimilarities in the nature of the chemical linkage could have influenced the liberation of MTX at the tumor tissue level.

In conclusion, the present results are encouraging, and further studies to assess the potential of this new class of chemotherapeutic agent are warranted. The mechanism underlying MTX is now being studied in different test systems. Thus, experiments are ongoing in which MTX and free bisphosphonate, as well as a mixture of the drug and free carrier, are administered in tumor-bearing mice. Moreover, these compounds will also be tested in a metastasis model where OHS tumors are growing in bone.

## Experimental protocols

*Chemistry*

Melting points were determined on a Kofler apparatus (heating block) and are uncorrected. $^{1}H$ and $^{13}C$-NMR spectra were recorded on a Jeol JNM FX 100 FT (100 MHz) or a Bruker AC 300 (300 MHz) spectrometer, in organic solvents ($CDCl_3$, $CD_3OD$, DMSO–$d_6$, *etc*) with either tetramethylsilane (TMS) ($\delta$ = 0 ppm), or $D_2O$ with the sodium salt of trimethylsilyl perdeuteropropanoic acid (TMPS) as internal standards ($\delta$ = 0 ppm). $^{31}P$-NMR spectra were recorded on a Jeol JNM FX 100 (100 MHz) instrument with $H_3PO_4$ (85% in $D_2O$) as an external standard ($\delta$ = 0 ppm).

Analytical thin-layer chromatography (TLC) was performed on silica-gel sheets (Merck, DC-Alufolien, Kieselgel, Germany; 60 $F_{254}$) or grafted silica-gel sheets (inverse phase) (DC-Fertig Platten; RP-18$F_{254}$S) and the plates were scanned under ultraviolet light, v = 254 nm; preparative column chromatography was run on silica gel 0.063–0.200 mm (Merck, 7734). Analytical HPLC was carried out on a Merck Hibar licrosphere 100 RP 8C 5 µm (250 x 4 mm) column with UV (254 nm) detection. Refractometry was measured on a Carl-Zeiss refractometer. Mass spectroscopy spectra were determined on a Hewlett–Packard 5995 gas chromatography/mass spectrometry.

Compounds were synthetized according to the procedures described: **1** [17], **2** [18], **4** [19], **6** [15] and **15** [20].

*Tetraethyl 3-ethoxycarbonyl-N-[4-(methylamino)benzoyl]-3-aminopropylidene-1,1-bisphosphonate 3*

To a stirred solution of 6.5 g (16 mmol) of **2** and 25 ml of triethylamine in 100 ml of THF at 0–5°C, 6.5 g (18 mmol) of **1** in 20 ml of THF was added and stirred at room temperature, for 1 h. The precipitate of triethylamine hydrochloride was separated by filtration. The filtrate was then evaporated to dryness, the residue was taken up in water and extracted with methylene chloride. Removal of the organic solvent gave an oil which was purified by chromatography on a silica-gel column (mobile phase ethylacetate/ethanol: 20/1) to give 8.0 g (70%) of compound **3** protected.

A solution of 1.3 g of $KH_3PO_4$ in 13 ml of water and 8 g of zinc powder, previously activated with an aqueous 5% HCl, was added to a solution of 6.5 g (9.1 mmol) of **3** N-protected in 80 ml of THF. The reaction mixture was then stirred at room temperature for 24 h. After filtration on cellite and evaporation of THF, the residue was taken up with water and extracted with chloroform. Removal of the solvent gave 4.9 g (quantitatively) of a colourless oil.

*Tetraethyl N-[4-[([2,4-diamino-6-pteridinyl]methyl) methyl-amino] benzoyl)-3-amino-3-ethoxycarbonylpropylidene-1,1-bisphosphonate* ***5***

To a stirred solution of 3.4 g (10 mmol) of **4** in 40 ml of DMA at 50°C, 5.9 g (11 mmol) of **3** in 5 ml of DMA was added. The reaction mixture was stirred at 50°C for 4 h and the solvent was evaporated. The brown viscous residue was then taken up with water and extracted with chloroform. Removal of the organic solvent gave a liquid residue which was crystallised from chloroform/diethylether to give 4.8 g (68%) of **5** as a yellow powder.

*Trisodium N-(4-[([2,4-diamino-6-pteridinyl]methyl)methylamino]-benzoyl)-3-amino-3-carboxylatopropylidene-1,1-bisphosphonate (compound* ***A****)*

To a stirred solution of 3.55 g (5 mmol) of **5** in 50 ml of methylene chloride, 4 ml (30 mmol) of trimethylsilyl bromide was added at 5°C. After stirring at room temperature for 48 h, the solvent was evaporated. The solid residue was dissolved in 100 ml of methanol and stirred at room temperature for 30 min. After removal of the solvent the phosphonic acid was precipitated from methanol with diethylether to give 3.0 g (5 mmol) of a pale yellow powder.

To this solid (5 mmol), 60 ml of ethanol was added and the solution was heated under reflux. Then 5 ml (17.5 mmol) of a 3.5 N NaOH aqueous solution was added dropwise and the reflux was maintained for 4 h. The precipitate was then filtrated and washed with ethanol and diethylether to give 3.19 g of compound as a clear yellow powder. NMR spectral data are reported in table II.

*N-[t-Butyloxycarbonyl]-L-glutamic acid -benzyl ester* ***7***

To a solution of 2.37 g (10 mmol) of **6** and 10 ml of 1 N NaOH in 20 ml of dioxane, a solution of 2.4 g (11 mmol) of *tert*-butylpyrocarbonate in 5 ml of dioxane was added dropwise at 0–5°C. The reaction mixture was then stirred for 30 min and the solvent was evaporated. The residue was taken up with water, the solution was made acidic (pH 2–3) with an aqueous solution of $KHSO_4$, and extracted twice with ethylacetate. Then the organic layers were washed with water. Removal of ethylacetate gave 3.3 g (98%) of a colourless oil which solidified at room temperature.

*$N^{\alpha}$-[t-Butyloxycarbonyl]-$N^{\delta}$-[1-ethoxycarbonyl-3,3-bis (diethylphosphono)propyl]glutamine benzyl ester* ***8***

To a solution of 2.0 g (5.9 mmol) of **7** in 100 ml of $CHCl_3$, a solution of 2.5 g (6.2 mmol) of **2** in 10 ml of $CHCl_3$ was added at 0°C. To this reaction mixture, a solution of 1.20 g (6.2 mmol) of dicyclohexylcarbodiimide in 20 ml of $CHCl_3$ was added dropwise, and stirring was maintained for 3 h. The solvent was then evaporated, the residue taken up in ethylacetate and the dicyclohexylurea separated by filtration. The organic filtrate was extracted with an aqueous solution of 5% $NaHCO_3$, then with an aqueous solution of 1 N HCl in order to eliminate unreacted acid and amine, respectively. Removal of the solvent gave 3.32 g (78%) of **8** as a colourless oil.

**Table II.** NMR spectral data of compound **A**.

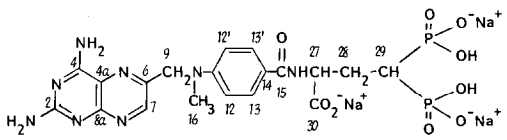

| *$^1$H-NMR (300 MHz)-$D_2O$* | *$^{13}$C-NMR (300 MHz)-$D_2O$* |
|---|---|
| $H_{28,29}$: 1.7–2.5; m; 3H | $C_{28}$: 31.9 |
| $H_{16}$: 3.2; s; 3H | $C_{29}$: 41.5 (t; $J_{C\text{-}P}$ = 130 Hz) |
| $H_{27}$: 4.3; m; 1H | $C_{16}$: 41.5 |
| $H_9$: 4.8; s; 2H | $C_9$: 57.9 |
| $H_{12,12'}$: 6.9; d; 2H | $C_{27}$: 61.8 |
| $H_{13,13'}$: 7.9; d; 2H | $C_{12,12'}$: 114.9 |
| $H_7$: 8.6; s; 1H | $C_{14}$: 124.2 |
| | $C_{4a}$: 125.2 |
| | $C_{13,13'}$: 132.2 |
| | $C_6$: 151.1 |
| | $C_7$: 152.1 |
| $^{31}$P-NMR (100 MHz)-$D_2O$ | $C_{11}$: 154.7 |
| | $C_4$: 156.3 |
| P: 20.36; s and 20.44; s | $C_2$: 165.0 |
| | $C_{8a}$: 165.8 |
| | $C_{15}$: 172.9 |
| | $C_{30}$: 183.8 |

*$N^{\delta}$-[1-Ethoxycarbonyl-3,3-bis(diethylphosphono)propyl] glutamine benzyl ester* ***9***

To a stirred solution of 2.17 g (3 mmol) of **8** in 10 ml of $CH_2Cl_2$, 15 ml of trifluoroacetic acid was added dropwise without noticing an increase in temperature. The reaction mixture was stirred for 20 min at 20°C. The solvent was evaporated, the residue taken up in 25 ml of ethylacetate and the pH (1–2) was increased by addition of an aqueous solution of $NaHCO_3$ cooled at 0°C, until pH 8–9. Then the organic layer was separated and washed with water. Removal of the solvent gave 1.7 g (90%) of **9** as a colourless oil.

*$N^{\alpha}$-[4-(Methylamino)benzoyl]-$N^{\delta}$-[2-ethoxycarbonyl-3,3-bis (diethylphosphono)propyl]glutamine benzyl ester* ***10***

Using the same procedure as described above for the synthesis of **3** N-protected, **10** N-protected was obtained (68%) after purification by chromatography on a silica-gel column (mobile phase: pure ethylacetate).

The subsequent removal of the trichloroethoxycarbonyl protecting group was operated analogously to **3** (quantitatively).

*$N^{\alpha}$-[4-[([2,4-Diamino-6-pteridinyl]methyl)methylamino]-benzoyl]-$N^{\delta}$-[1-ethoxycarbonyl-3,3-bis(diethylphosphono)-propyl]glutamine benzyl ester* ***11***

Using the same procedure as described for the synthesis of **5**, **10** reacted with **4** to give **11** (61%).

*Pentasodium salt of $N^{\alpha}$-[4-[([2,4-diamino-6-pteridinyl] methyl)-methylamino]benzoyl]-$N^{\delta}$-[1-carboxylato-3,3-bis(phosphonato) propyl] glutamine (compound **B**)*
Using the same silylation conditions as described for compound **A**, **11** yielded the phosphonic acid quantitatively as a yellow powder.

To 5.3 g (5.4 mmol) of this solid, 20 ml methanol was added and the solution was heated under reflux. Then 37.8 ml (37.8 mmol) of a 1 N NaOH aqueous solution was added dropwise and the stirring was maintained at 75°C for 8 h. The solution was then concentrated. The salt was precipitated with methanol and washed with diethylether to give 4.2 g (97%) of compound **B** as a yellow powder. NMR spectral data are reported in table III.

*N-[t-Butyloxycarbonyl]-L-glutamine **13***
To a stirred solution of 2.92 g (20 mmol) of L-glutamine in 40 ml of dioxane and 20 ml of water, 20 ml of 1 N NaOH was added and solubilisation occurred. Then 4.6 g (2 mmol) of tertiobutylpyrocarbonate in 10 ml of dioxane was added at 0°C, and stirring was maintained for 1 h at room temperature. Solvents were evaporated and the white, half solid, residue was taken up in 50 ml of water. The pH (8–9) was lowered to pH 2–3 by addition of an aqueous solution of $KHSO_4$. Two extractions with ethylacetate, washing of the organic layers with water and removal of the solvent, gave 3.4 g (70%) of **13** as a white half-solid.

**Table III.** NMR spectral data of compound **B**.

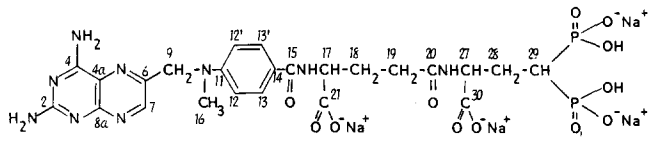

| *$^1$H-NMR (300 MHz)-$D_2O$* | *$^{13}$C-NMR (300 MHz)-$D_2O$* |
|---|---|
| $H_{18,19,28,29}$: 1.8–2.5; m; 7H | $C_{18+28}$: 30.8 |
| $H_{16}$: 3.1; s; 3H | $C_{19}$: 35.1 |
| $H_{17+27}$: 4.2–4.3; m; 2H | $C_{29}$: 39.0 (t; $J_{CP}$ = 112 Hz) |
| $H_9$: 4.7; s; 2H | $C_{16}$: 41.5 |
| $H_{12,12'}$: 6.8; d; 2H | $C_9$: 57.1 |
| $H_{13,13'}$: 7.7; d; 2H | $C_{27}$: 58.3 |
| $H_7$: 8.5; s; 1H | $C_{17}$: 59.2 |
| | $C_{12,12'}$: 113.8 |
| | $C_{14}$: 126.6 |
| | $C_{4a}$: 124.5 |
| $^{31}$P-NMR (100 MHz)-$D_2O$ | $C_{13,13'}$: 131.3 |
| | $C_6$: 150.3 |
| P: 19.3; s | $C_7$: 151.4 |
| | $C_{11}$: 153.7 |
| | $C_4$: 155.6 |
| | $C_2$: 164.3 |
| | $C_{8a}$: 164.9 |
| | $C_{15}$: 171.5 |
| | $C_{20}$: 178.5 |
| | $C_{21}$: 181.6 |
| | $C_{30}$: 182.9 |

*N-[t-Butyloxycarbonyl]-L-glutamine ethyl ester **14***
A mixture of 3.4 g (13.8 mmol) of **13**, 1.23 ml (14.5 mmol) of ethyliodide and 2.7 ml (14,5 mmol) of diisopropyethylamine in 25 ml of dioxane was stirred for 4 days at room temperature. Then the solvent was evaporated, the residue taken up with water and twice extracted with ethylacetate. Removal of the solvent, precipitation with ethylacetate/petroleum ether and crystallisation from ethanol gave 3.2 g (94%) of **14** as a white solid.

*$N^{\alpha}$-[t-Butyloxycarbonyl]-$N^{\delta}$-[2,2-bis(diethylphosphono) ethyl]glutamine ethyl ester **16***
To a stirred solution of 0.1 g (1 mmol) of potassium tertiobutylate in 50 ml of tertiobutanol, 2.74 g (10 mmol) of **14** was added at 50°C. Solubilisation occurred rapidly and **15** was added dropwise. The reaction mixture was stirred for 1 h at 50°C. The pH was made neutral by addition of a saturated aqueous solution of $NH_4Cl$. Extraction with $CH_2Cl_2$ and removal of the solvent gave 5.2 g (90%) of **16**.

*$N^{\delta}$-[2,2-bis(Diethylphosphono)ethyl]glutamine ethyl ester **17***
To a stirred solution of 2.0 g (3.5 mmol) of **16** in 15 ml of $CH_2Cl_2$, 25 ml of trifluoroacetic acid was added and the reaction mixture was stirred for 20 min. The solvent was evaporated and the residue taken up in an aqueous solution of 5% $NaHCO_3$ (pH 8–9). Two extractions with $CH_2Cl_2$ followed by removal of the solvent gave 1.2 g (70%) of **17**.

*$N^{\alpha}$-[4-(Methylamino)benzoyl]-$N^{\delta}$-[2,2-bis(diethylphosphono) ethyl)glutamine ethyl ester **18***
Synthesis of **18** N-protected (68%) was performed using the same procedure as described for **3** N-protected.

The subsequent removal of the trichloroethoxycarbonyl protecting group was identical to that of **3** (quantitatively).

*$N^{\alpha}$-[4-[([2,4-Diamino-6-pteridinyl]methyl)methylamino] benzoyl]-$N^{\delta}$-[2,2-bis(diethylphosphono)ethyl]glutamine ethyl ester **19***
Using the same procedure as described for the synthesis of **5**, **18** reacted with **4** to give **19** (70%).

*Tri-sodium salt of $N^{\alpha}$-[4-[([2,4-diamino-6-pteridinyl]methyl) methylamino]benzoyl]-$N^{\delta}$-[2,2-bis(phosphonato) ethyl] glutamine (compound **C**)*
Using the same silylation and saponification conditions as described for the conversion of **5** to A, **19** gave **C** (quantitatively). NMR spectral data are reported in table IV.

*Pharmacological evaluation*

*Animals*
Both male and female nude mice of different background (BALB/c nu/nu, NIH III nu/nu) were used. Mice were kept under specified pathogen-free conditions. Food and water were supplied *ad libitum*.

*Tumor lines*
Selection of human osteosarcoma lines was based on in histology, growth characteristics and sensitivity to established cytostatic drugs, if known. Details on the characterization of tumor

**Table IV.** NMR spectral data of compound **C**.

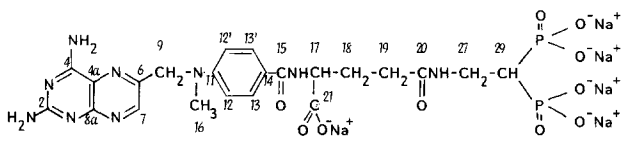

| *$^1$H-NMR (300 MHz)-$D_2O$* | *$^{13}$C-NMR (300 MHz)-$D_2O$* |
|---|---|
| $H_{18,19,27,29}$: 1.5–2.6; m; 7H | $C_{18}$: 27.9 |
| $H_{16}$: 3.3; s; 3H | $C_{19}$: 32.8 |
| $H_{17}$: 4.5; m; 1H | $C_{29}$: 40.2 (t; $J_{CP}$ = 112 Hz) |
| $H_9$: 5.0; s; 2H | $C_{16}$: 40.2 |
| $H_{12,12'}$: 6.8; d; 2H | $C_{27}$: 51.8 |
| $H_{13,13'}$: 7.8; d; 2H | $C_{9+17}$: 57.4 |
| $H_7$: 8.5; s; 1H | $C_{12+12'}$: 112.1 |
| | $C_{14}$: 124.7 |
| $^{31}$P-NMR (100 MHz)-$D_2O$ | $C_{4a}$: 125.9 |
| | $C_{13+13'}$: 132.0 |
| P: 20.14; s and 20.26; s | $C_6$: 147.8 |
| | $C_7$: 153.8 |
| | $C_{11}$: 154.1 |
| | $C_4$: 157.9 |
| | $C_2$: 164.8 |
| | $C_{8a}$: 166.0 |
| | $C_{15}$: 169.5 |
| | $C_{20}$: 176.2 |
| | $C_{21}$: 181.8 |

cell line OHS and the xenograft model have been reported previously [21]. Human tumor xenograft TTX was established in nude mice from a primary osteosarcoma of a patient at the Norvegian Radium Hospital (Oslo).

*In vivo antitumor activity studies*

Human tumor xenografts were studied as subcutaneous implants in both flanks of nude mice. Tumor growth was assessed weekly by caliper measurements of the tumor in two dimensions [22, 23]. Treatment was started in a randomized fashion when tumors had reached a median tumor diameter of 5–6 mm; tumors smaller than 4 mm in diameter (or minimum volume of 30 $mm^3$) at the start of treatment were excluded from the final analysis. Each treatment group and control group consisted of 5–8 mice bearing in total 5–14 evaluable tumors. Prior to the start of treatment, mice were selected according to tumor sizes and assigned to groups in order to obtain an equal distribution of tumor volumes in the different groups.

Tumor volume was calculated according to the formula 0.5 x length x width$^2$. Relative tumor volumes (RTV) were calculated for each single tumor by dividing the tumor volume on day X by the tumor volume on day 0 at the start of treatment:

$$RTV = \frac{\text{Volume tumor day X}}{\text{Volume tumor day 0}} \times 100$$

Median RTV values were used for drawing growth curves and calculating treatment efficacy. Tumor doubling time (TD) of test and control groups was defined as the period required to reach a median RTV of 200 and 400%.

Treatment efficacy was assessed by three evaluation criteria used in parallel: specific growth delay (SGD), optimal growth inhibition (T/C %) and tumor growth curve [23]. The SGD was calculated with regard to the TD of test and control groups:

$$SGD = \frac{\text{TD treated} - \text{TD control}}{\text{TD control}}$$

Optimal growth inhibition (T/C %) was calculated with regard to the RTV of treated groups *versus* control:

$$T/C\% = \frac{\text{RTV treated}}{\text{RTD control}} \times 100\%$$

*Determination of the maximum tolerated dose*

Drugs were administered to tumor-bearing nude mice at equitoxic dose levels allowing a median body weight loss of 10–15% and toxic death in one-third of the animals per treatment group. Toxic death was defined as death within 2 weeks after final drug injection.

Prior to the start of the main study, dose-finding studies in non-tumor-bearing nude mice were carried out in order to determine the maximum tolerated dose (MTD) for each drug (iv, day 0 and 7).

*Drugs*

For *in vivo* administration compounds **1**, **B** and **C** were solubilized and diluted in Locke (NaCl 7.6 g, KCl 0.42 g, $CaCl_2$ 0.24 g, $NaH_2PO_4$ 0.143 g, $NaHCO_3$ 2.1 g and glucose 2 g per liter water, pH 7.5) and occasionally in 0.9% NaCl. MTX was used in 0.9% NaCl.

*Drug treatment*

Each treatment group consisted of 5–8 tumor-bearing nude mice. The following groups were studied: 1) control; 2) compound **A**, iv day 0 and 7, 100 mg/kg/injection; 3) compound **B**, iv day 0 and 7, 75–60 mg/kg/injection or 100–75 mg/kg/injection or 50–50 mg/kg/injection; 4) compound **C**, iv day 0 and 7, 75–75 mg/kg/injection; 5) MTX, ip day 0 and 7, 150–150 mg/kg/injection or 200–200 mg/kg/injection.

## Acknowledgments

We wish to thank ARC (Commision Scientifique Grand Ouest) and the Foundation Langlois for financial support.

## References

1 Jaffe N (1972) *Cancer* 30, 1627–1630
2 Rosen G (1985) *Orthopedics* 8, 659–664
3 Jaffe N (1986) *Cancer Update* 82, 42–44
4 Bleyer WA (1978) *Cancer* 41, 36–51
5 Jung A, Bisaz S, Fleisch H (1973) *Calcif Tissue Res* 11, 269–280
6 Fleisch H (1989) *Recent Results Cancer Res* 116, 1–28
7 Ralston SH, Alzaid AA, Gallacher SJ, Gardner MD, Cowan RA, Boyle IT (1988) *Q J Med* 69, 825–834

8 Burckhardt P, Thiebaud D, Perey L, von Fliedner V (1989) *Recent Results Cancer Res* 116, 54–66
9 Wingen F, Sterz H, Blum H, Möller H, Pittermann W, Pool BL, Sinn HJ, Spring H, Schmähl D (1986) *J Cancer Res Clin Oncol* 111, 209–219
10 Sturtz G, Voisin-Dacheux P, Guillamot G (1990) *CR Acad Sci Paris* t 310, sér II, 739–742
11 Jolivet J, Cowan KH, Curt GA, Clendenin NJ, Chabner BA (1983) *N Engl J Med* 309, 1094–1104
12 Piper JR, Montgomery JA (1977) *J Org Chem* 42, 208–211
13 Nair MG, Baugh CM (1973) *Biochem* 12, 3923
14 McKenna CE, Higa MT, Cheung NH, McKenna MC (1977) *Tetrahedron Lett* 2, 155
15 Sachs H, Brande E (1953) *J Am Chem Soc* 75, 4610–4611
16 Kjonniksen J, Nesland JM, Pihl A, Fodstad O (1990) *J Natl Cancer Inst* 82, 408–412
17 Windholz TB, Johnston DBR (1967) *Tetrahedron Lett* 27, 2555–2557
18 Sturtz G, Guervenou J (1991) *Synthesis* 8, 661–662
19 Piper JR, Montgomery A (1977) US Pat 4,077,957
20 Voisin-Dacheux P (1987) Ph D Thesis, UBO Brest
21 Fodstad O, Brogger A, Bruland O, Solheim OP, Nesland JM, Pihl A (1986) *Int J Cancer* 38, 33–40
22 Fodstad O, Aamdal S, McMenamin M, Nesland JM, Pihl A (1988) *Int J Cancer* 41, 442–449
23 Boven E, Winograd B, Fodstad O, Lobbezoo NW, Pinedo HM (1988) *Eur J Cancer Clin Oncol* 42, 567–573